Optimizing Max Camber Points Along Thin Triangular Airfoils for Higher Lift/Drag Ratios

By A. Henn[1] and K. Stameski[2]
Florida Institute of Technology, Melbourne, FL, 32901, USA

The purpose of this report is to expand knowledge on the lift and drag properties of thin triangular airfoils, and determine whether or not they are a viable option for low-Reynolds number applications. Thin triangular airfoils were thought to be more efficient than standard NACA airfoils under specific conditions. This experiment was performed through the wind tunnel testing of a NACA 2412 and nine thin triangular airfoils with varying max camber points. Between the Reynolds numbers of 30-42,000, lift and drag values were collected at varying angles of attack. Overall, it was found that the thin triangular airfoils proved to have unique lift and drag characteristics when compared to the standard NACA 2412.

I. Nomenclature

A	=	frontal projected area	Re	=	Reynolds number
C_d	**=**	coefficient of drag	S	=	wing area
C_l	=	coefficient of lift	t	=	airfoil thickness
c	=	chord	U	=	air velocity
D	=	force due to drag	α	=	angle of attack
h	=	height of airfoil	ε	=	blockage
h_t	=	height of wind tunnel test section	ν	=	kinematic viscosity
L	=	force due to lift	ρ	=	air density
M	=	pitching moment	σ	=	streamline curvature

II. Introduction

The aerodynamic characteristics of an airfoil depend on its environment and its shape. In real-world applications, a higher lift-to-drag ratio is preferred for airfoils, because it leads to more efficiency in steady-level-flight. Efficiency is crucial in extending performance capabilities, such as flight endurance and range of an aircraft. By design, airfoils are meant to operate most efficiently at specific Reynolds numbers (Re#s). Conventionally, they are not designed for low Re# applications. On the other hand, thin triangular airfoils (TTAs) behave differently than conventional NACA airfoils, and their simple and variable construction can make a viable airfoil for low Re#s.

Low Re# applications include; low flying small, uncrewed aerial vehicles (UAVs) and Martian surface UAVs. Wind tunnel testing is an option to find the aerodynamic characteristics of airfoils at such low Re#s. Varying wings with TTAs were 3-D modeled and printed to be tested in a wind tunnel. Florida Institute of Technology's Experimental Aerodynamics Laboratory's Jetstream 500 wind tunnel was operated at a Re# range of 30-42,000;

---

with increments of 3,000 between. In order to optimize the lift and drag properties of TTAs, nine different wings were printed, and a NACA 2412 wing was used as a control. In order to only test one changing variable on the airfoil design, a methodology had to be used to keep them consistent. The nine TTAs had matching geometries, aside from the location of the max camber point along the chord. To match the Re# range, the wings' chord lengths were always 50 mm. Separately, to keep consistency, the heights of the tested 3-D models were always 5 mm.

Each wing/airfoil test yielded data in the form of lift and drag; both in lbf, and wind speed; in mph. Varying angles of attack (AoAs) from 0 to 20 degrees, with increments of 5 degrees, were tested for a total of 50 trials. After unit conversions, raw data was plotted into both lift and drag vs. velocity curves, respectively. Trendline analysis was performed to determine the lift and drag values at specific velocities corresponding to selected Re#. These force values were used in calculations to find uncorrected coefficients of lift and drag for each airfoil. Finally, correction calculations according to the specifications of the Jetstream 500 were performed to determine the true coefficients of lift and drag. The final values for lift and drag were used to find the L/D, providing a measurement of overall efficiency of the TTAs.

Further theory in the form of mathematical equations is found in the section below (III. Theory). More in-depth descriptions of TTAs and the laboratory and the results are presented in the subsequent sections (IV. Experimental Setup and V. Results).

III. Theory

Airfoils come in two forms: symmetrical and asymmetrical. Symmetrical airfoils only generate lift when at a positive AoA, and asymmetrical airfoils are capable of generating lift at zero, or even lower, AoAs. This is achieved with a design element known as the "camber." It allows the airfoil and its wing to generate lift by compressing passing streamlines when in movement. The relative wind on the upper portion of the airfoil is accelerated by this cross-sectional compression more than that of the bottom. This leads to a pressure gradient with lower pressure on the top of the wing that pushes the wing upwards. This force-due-to-pressure is known as "lift."

Another force acting on wings is "drag." Drag is a fundamental non-conservative force that resists movement in a fluid, like air. Drag is caused primarily by skin friction and its ensuing momentum transfer. Skin friction is the tendency of fluid particles to stagnate along the surface of the wing. This stagnation effect leads to a momentum transfer in the opposite direction of flight, causing the flying body to lose kinetic energy.

Both lift and drag forces are calculated with lift and drag equations, Eq. (1) and (2) respectively. Each figure has a corresponding coefficient: C_l and C_d. In general, at higher AoAs, these coefficients both increase leading to a higher lift force; but at the same time, more force-due-to-drag is present. At a certain point, if the AoA continues to be increased, the wing will "stall" and lose almost all lift, breaking the trend of positive lift to AoA.

$$L = \tfrac{1}{2}\rho U^2 S C_l \qquad\qquad (1)$$

$$D = \tfrac{1}{2}\rho U^2 A C_d \qquad\qquad (2)$$

It is worth noting that both forces behave very similarly and they increase exponentially with velocity. These can be reordered to derive the coefficients of lift and drag. Found below, Eq. (3) contains both of these coefficients, as they contain the same variables other than L and D:

$$C_{l,u} = \frac{2 \cdot L}{\rho U^2 S} \;,\; C_{d,u} = \frac{2 \cdot L}{\rho U^2 A} \qquad\qquad (3)$$

The preceding formulas are used to find the lift and drag coefficients in wind tunnels tests, as they rely on values known, such as air density, velocity, and wing area. However, they are uncorrected for certain factors, such as "solid/wake blockage" and "streamline curvature." Solid blockage is caused by a reduction in the cross-sectional area of the wind tunnel test section by the presence of the airfoil for the test. This constriction of the test section causes the wind to accelerate to a higher velocity than set by the computer, requiring compensation to avoid error. Formulas for solid blockage correction with and without AoA are found below in Eq. (4) and (5), respectively:

$$\varepsilon_{sb_{w/AoA}} = \varepsilon_{sb_0}\left(1 + 1.1\frac{c}{t}\alpha^2\right) \quad\quad (4)$$

$$\varepsilon_{sb_{0,\,w/o\,AoA}} = \frac{\pi}{6}\left(1 + 1.2\frac{t}{c}\right)\left(\frac{A}{h_t^2}\right) \quad\quad (5)$$

Wave blockage produces similar effects during wind tunnel tests. It is a result of the compression and directional change of streamlines in the wind tunnel, when the wind flows around the airfoil. The subsonic compression of oncoming wind creates a weak cone that could be considered another solid body. Even at low Mach numbers, where compressibility is rather low, it can be accounted for. This compensation is found as Eq. (6):

$$\varepsilon_{wb} = \frac{1}{4}\frac{c}{h_t}C_{d,u} \quad\quad (6)$$

Wave and solid blockage are combined to form total blockage in Eq. (7):

$$\varepsilon = \varepsilon_{sb} + \varepsilon_{wb} \quad\quad (7)$$

Lastly, the streamline curvature correction accounts for directional streamline changes parallel to the concave and convex surfaces protruding from the top and bottom surfaces along the chord of the airfoil. This causes pressure differentials along the surface of the wing, and it is accounted for with the formula shown in Eq. (8) below:

$$\sigma = \frac{\pi^2}{48}\left(\frac{c}{h_t}\right)^2 \qu\quad (8)$$

These formulas come together to provide the corrected lift and drag coefficients for each airfoil. They are found below in Eq. (9) and (10), respectively:

$$C_l = C_{l,u}(1 - \sigma - 3\varepsilon) \quad\quad (9)$$
$$C_d = C_{d,u}(1 - 3\varepsilon_{sb} - 2\varepsilon_{wb}) \quad\quad (10)$$

An essential value to understanding the design of airfoils and wings is the Re#. A non-dimensional quantity, the Re# is best described as an indicator as to whether or not a flow will be laminar or turbulent and if originating as laminar flow, it defines relatively how soon the flow will become turbulent. The higher the Re#, the more likely a flow will be turbulent. In general, laminar flow is preferred around a wing, because turbulent flow leads to lower pressure, which on the bottom surface will decrease the overall lift, and on the top surface will increase stall-inducing drag. In the case of airfoils, the Re#, being a function of velocity and chord length seen in Eq. (11), acts as a scaling factor:

$$Re\# = \frac{Uc}{v} \quad\quad (11)$$

For example, commercial jets fly at very high Re#'s, likely in the 100k-10mil range; slower-flying sea-level recreational UAVs fly at a range of around Re# = 30k-100k. Specific aircraft depend on a wide variety of airfoils to produce lift in their wings; and each airfoil must be designed to perform best, depending on the Re# scaling in question. Therefore, it is essential for aeronautical engineers to select proper airfoils to operate at certain Re#s.

TTAs are designed to function best at lower Re#s, generally under 100k. At this scale, any wing in flight is interacting with comparatively larger fluid particles that do not as easily form to the surface. It is this fact that sets the TTA apart from purely convex airfoils, like NACA-standard airfoils. At higher Re# ranges, the leading edge plate would normally act as a flat plate-wing pitched down relative to oncoming wind, making negative lift because the overall pressure under the wing is lower than the top surface. However, at a lower Re# range, the more laminar streamlines will not allow vortices to build behind the leading edge plate under the wing, keeping a preferable pressure gradient, seen in other wings.[1]

IV. Experimental Setup

TTAs are based on a long flat triangle with the bottom edge and inside area removed. This leads to TTAs being asymmetric, and the defining geometries are based on ratios of the max camber point and height. Similar to NACA airfoils, for easy referencing, a naming convention was developed for the airfoils tested. An example of the naming convention in use is "TTA-2010"; pictured below in Fig. 1:
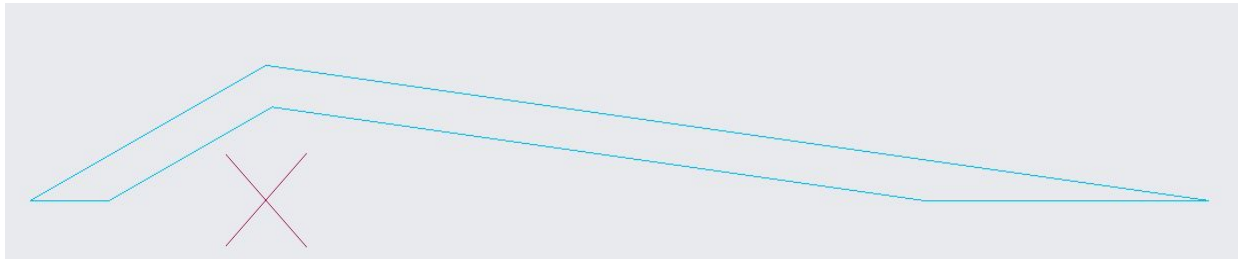

Fig. 1 An engineering drawing of the TTA-2010 airfoil. Notice, the cross mark denotes the location of the max camber point.

In this, the "TTA" stands for "thin triangular airfoil," and the first two digits describe the location of the max camber point along the chord as a percentage of the chord itself. The third and fourth digits describe maximum height of the airfoil, also as a percentage of the chord. As previously stated, nine TTAs were designed and tested along a range of max camber point positions, starting from 10% going to 50%, in increments of 5%.

A. Design & Printing

The fundamental construction of a TTA-based wing involves joining two flat plates along one edge; the leading plate sloped upwards relative to oncoming wind, and the trailing plate sloped downwards from the joining edge. In order to achieve this, 3-D modelling software was implemented. To keep the design of the airfoils consistent, allowing a change of only max camber point location, a triangle was used as the outline of each airfoil; pictured below in Fig. 2. The top angle of this shape became the max camber point, and its location was determined as a ratio of the chord length. The bottom edge of the triangle became the airfoil's chord line.
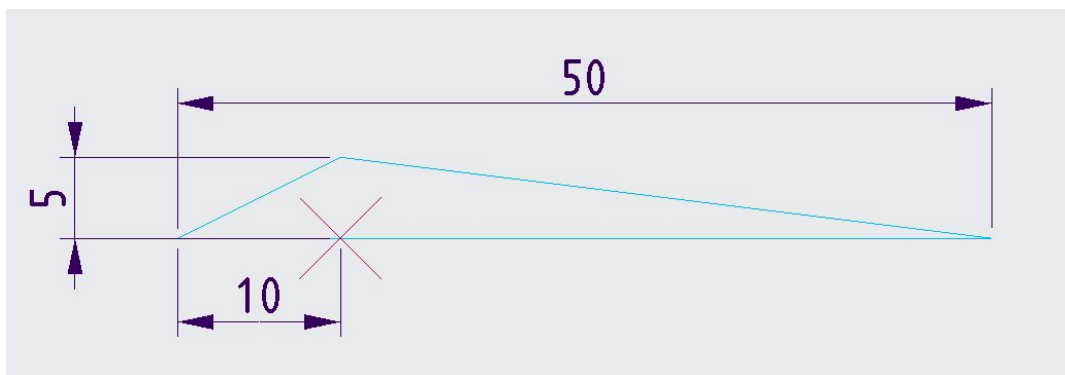

Fig. 2 An engineering schematic of the triangle used to create the TTA-2010. As the naming convention suggests, the max camber point is located at 20% of the chord length and the height is 10% of the chord length.

Seen below in Fig. 3, rectangles were drawn from the top sides of the triangle. This is to create the airfoil's thickness. The thickness was kept at 1.5 mm due to 3D printing restrictions. Any material below the chord line is cut to flatten the bottom edges, cutting the rectangles. This was done to keep the design consistent and keep the height based on the original triangle.
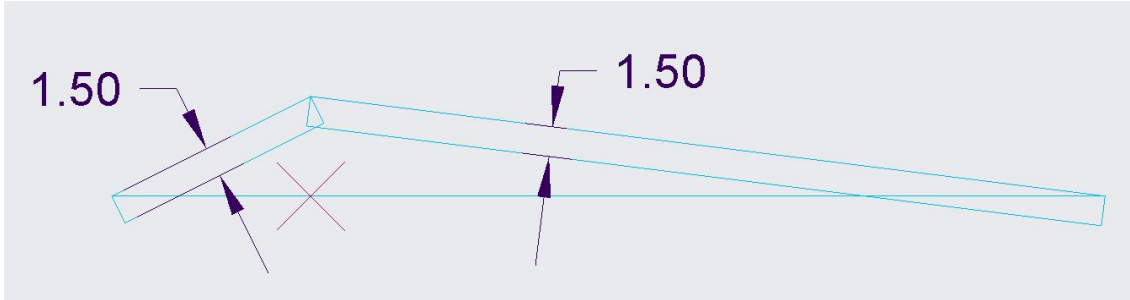
Fig. 3 An engineering drawing depicting the leading and trailing rectangles

The most important dimensions of the TTAs are the chord lengths. For the purposes of the following experiment, a chord of 50 mm and width of 120 mm was chosen for all wings, including the NACA 2412, because it allowed the capabilities of the wind tunnel to line up with the intended Re# range. On the underside of each wing, a flat connection point parallel to the chord was required to join the individual airfoils to the wind tunnel's force sensor, during testing. Fig. 4 depicts this below:
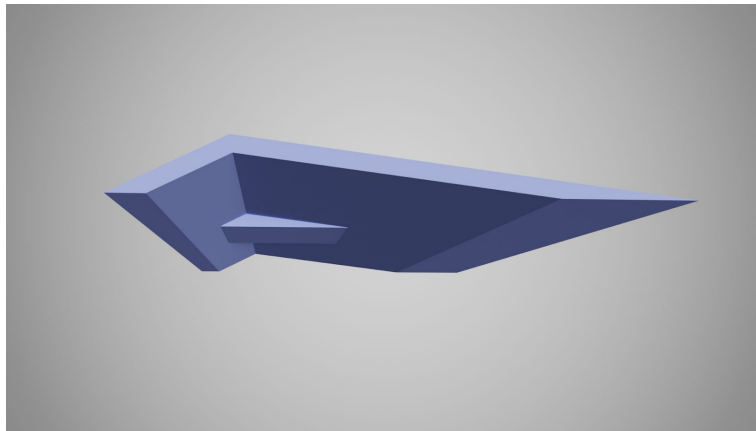

Fig. 4 An underside rendering of a TTA.

B. Equipment

A Jetstream 500 wind tunnel and accompanying software were used in data collection for the ten airfoils. A TTA is pictured in the wind tunnel test section in Fig. 5 below:

Fig. 5 A TTA in the Jetstream 500 wind tunnel.

V. Results

An independent variable in question was the max camber position. As the max camber point of a TTA is moved away from the leading edge, the lift/drag characteristics change dramatically where there is not an obvious pattern as shown in Fig. 6 below. The purpose of displaying a chaotic graph is to show that when a TTA is varied by max camber point, the result is an extremely wide range of performance. Even inconsistency is important to investigate, because the lack of patterns on the graph shown provide important information. Changing max camber point of a TTA does not linearly change C_l over C_d. To accurately predict how a TTA will perform, a different variable must be chosen that keeps max camber point the same.
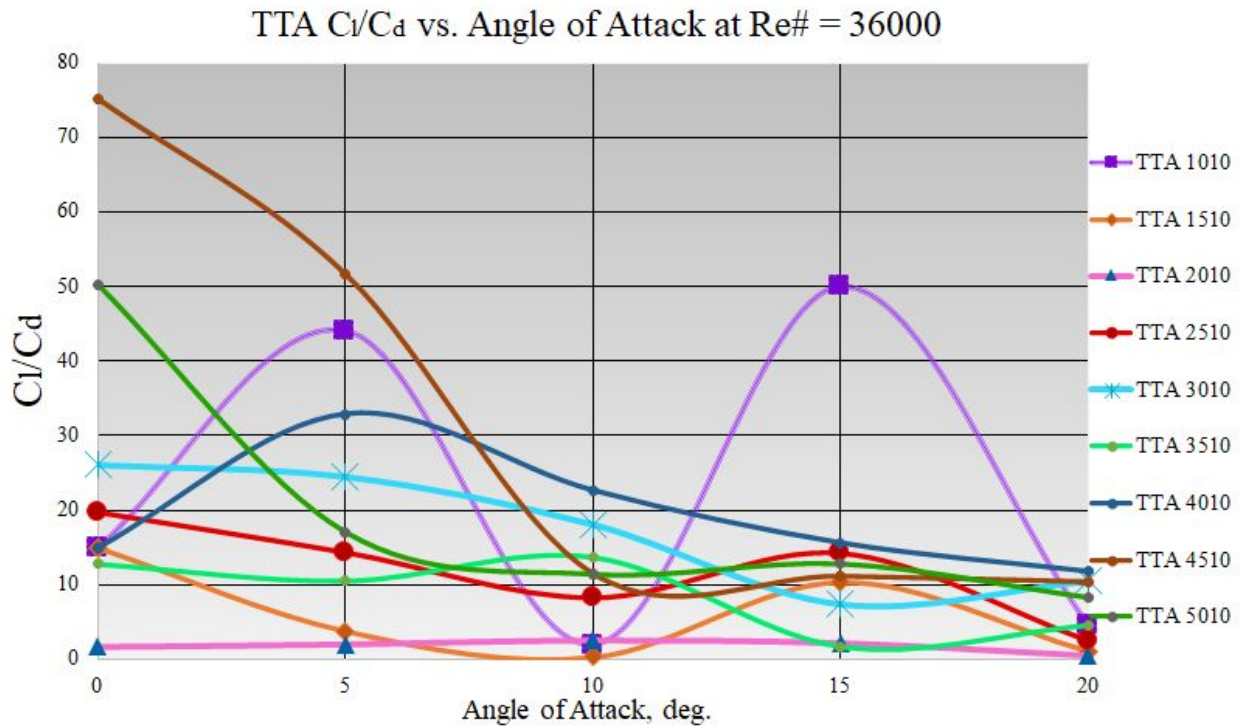

Fig. 6 Graph of each airfoil tested at a single Re#

Changing the position of the max camber point along the TTAs' chords changed the performance of the airfoils differently at each AoA. The lift/drag relationship presented in the final data is surprisingly volatile in how the airfoil can seemingly stall before being more efficient at a more aggressive AoA. Testing showed peak efficiencies to be at these varying AoAs. For example, the TTA-3510 showed a peak L/D at 10 degrees, while the TTA-1010 peaked at 5 and 15 degrees. Fig. 7 depicts this relationship below:
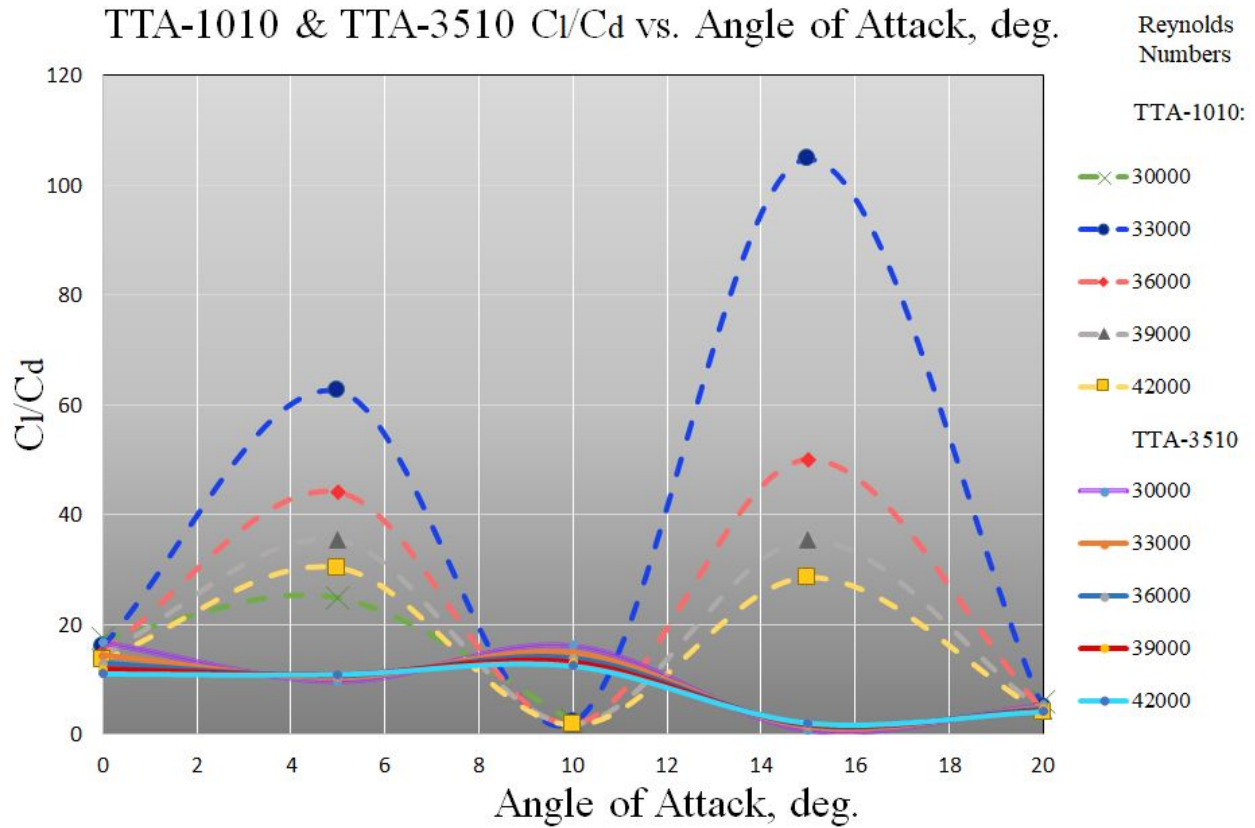
Fig. 7 Graph comparing TTA-1010 and TTA-3510

The most consistent pattern shared by the TTAs is that lower Re# yielded higher L/Ds. TTAs with max camber points at 25-50% of their chords perform more efficiently as the Re# decreases. This property is illustrated most prominently in the TTA-2510 plot depicting C_l over C_d vs. AoA in Fig. 8 below. The increasing efficiency of the TTAs as Re# decreases could mean a peak efficiency at much lower Re# beyond the scope of testing. The nearly concentric lines that the graph shows between 0 and 20 degrees AoA somewhat verifies that the lines shown truly depict the airfoils' performance. This pattern is also shown in the sample NACA-2412.
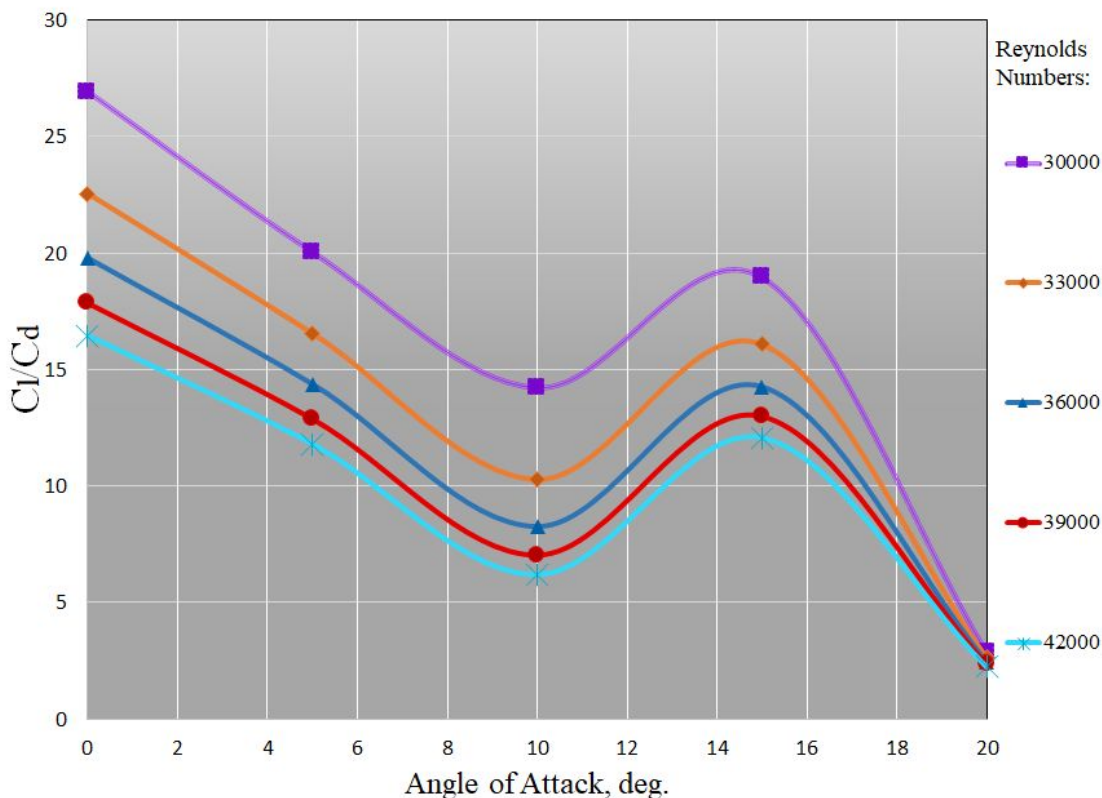
Fig. 8 Graph showing final TTA-2510 final, corrected data

As the theory suggests, TTA-based wings still functioned the way other positive-camber airfoils would, by providing a lift force in the presence of oncoming wind. Although some examples of lift vs. AoA curves provided jagged trends, a positive slope was still present in the majority of tests, proving that whether or not TTAs are more efficient than NACA airfoils at low Re#s, they still can be considered viable airfoils for whatever niche they are found to be useful in.

VI. Further Discussion

The research covered in this paper leads to further questions about the properties of TTAs. TTAs are unique in their simplicity, flight characteristics, and potential adaptability. Further research is needed to expand knowledge on how TTAs perform in different conditions, as well as how changing aspects of TTAs can influence its properties.

To begin to understand how such airfoils can be utilized, more research is needed to expand the scope of testing to include lower Re#s and negative AoAs, as well as a smaller increment between these angles of attack. Reducing the increments between AoAs would provide a higher degree of confidence that the airfoil will perform as the charts show. The negative AoAs would need to be tested before utilization so that we could predict how the airfoil will perform during a dive. Future research could utilize testing equipment such as depressurized wind tunnels or water tunnels that can more accurately imitate lower Re# flows. Computer simulation could be used in future experiments to verify the results as well as provide a larger set of data.

The simple shape of a TTA could allow wing fabrication to be significantly different than traditional airfoil wing fabrication. The shape of a possible wing could possibly allow collapsing or folding where the plates join. The triangular shape inherently prevents wing flex if the leading and trailing edge are tethered; a TTA-based wing may not require a skin layered over a support structure, but instead two flat plates connected at a joint. Further testing could discover how lift devices could affect the performance

VII. Conclusion

Changing their max camber point locations of the nine TTAs tested allows a situational optimization to NACA airfoils in the low Re# range. The way this change affected the lift/drag ratio was shown individually, but a pattern could not be determined to help predict how other TTAs with different max camber points perform outside the scope of testing. It can be concluded that TTAs are designed to operate at lower Re#s, because most of the TTAs' lift/drag curves were trending towards a peak at less than Re# = 30,000. Each change in max camber point location provided a unique lift/drag curve that could be favorable situationally.

Acknowledgments

References

[1]Hidaka, H., and Okamoto, M., "An Experimental Study of Triangular Airfoils for Mars Airplane," Original Paper, Graduate School, Kanazawa Institute of Technology, and Kanazawa Institute of Technology, Nonoichi, Japan, 2013